



## Pathological mechanism of musculoskeletal manifestations associated with CRPS type II: An animal study



Hideyuki Ota\*, Tetsuya Arai, Katsuyuki Iwatsuki, Hideki Urano, Toshikazu Kurahashi, Shuichi Kato, Michiro Yamamoto, Hitoshi Hirata

Department of Hand Surgery, Graduate School of Nagoya University, Nagoya, Japan

Sponsorships or competing interests that may be relevant to content are disclosed at the end of this article.

### ARTICLE INFO

#### Article history:

Received 5 November 2013

Received in revised form 8 May 2014

Accepted 19 June 2014

#### Keywords:

Allodynia

Animal experiment

Complex regional pain syndrome

Contracture

Musculoskeletal manifestations

Pain

### ABSTRACT

Patients with complex regional pain syndrome (CRPS) often complain of abnormal sensations beyond the affected body part, but causes of this spread of musculoskeletal manifestations into contiguous areas remain unclear. In addition, immobilization can predispose to the development of CRPS. We examined functional, biochemical, and histological alterations in affected parts, including contiguous zones, using an animal model. Ten-week-old male Wistar rats were assigned to 5 groups: a normal group receiving no treatment, a sham operation group with surgical exploration, an immobilization group with surgical exploration plus internal knee joint immobilization, a surgical neuropathy group prepared by spinal nerve ligation (SNL) of the left L5 nerve root, and a surgical neuropathy + immobilization group with simultaneous SNL and knee joint immobilization. Mechanical allodynia and knee contracture were compared between groups, and tissues were harvested for histological assessments and gene and protein expression analyses. Neither surgical procedures nor immobilization induced detectable mechanical sensitivity. However, the addition of nerve injury resulted in detectable mechanical allodynia, and immobilization not only accelerated hyperalgesia, but also resulted in muscle fibrosis. Nerve growth factor (NGF) and other mediators of neurogenic inflammation were highly expressed not only in denervated muscles, but also in innervated muscles in contiguous areas, suggesting the spread of NGF production beyond the myotome of the injured nerve. Transforming growth factor  $\beta$  was involved in the development of contracture in CRPS. These findings imply that neuroinflammatory components play major roles in the progression and dispersion of both sensory pathologies and pathologies that are exacerbated by immobilization.

© 2014 International Association for the Study of Pain. Published by Elsevier B.V. All rights reserved.

## 1. Introduction

Complex regional pain syndrome (CRPS) type II is an extreme form of neuropathic pain that also affects functions of the autonomic nervous system, the motor regulatory system, and even the musculoskeletal system. Affected patients often complain of abnormal sensations beyond the affected body part. Close observation of such patients frequently reveals associations with movement disorders such as dystonia or musculoskeletal manifestations such as joint contracture in the involved areas.

This mysterious dispersed distribution has historically been viewed by neurologists and psychiatrists in the context of a

psychogenic origin [16,29,36]. However, recent research has been accumulating evidence that neuroinflammatory components play critical roles in the onset and progression of CRPS [30]. In a study of adult CRPS patients, 90% showed autoantibodies to either the  $\beta$ 2-adrenergic receptor ( $\beta$ 2AR) or the muscarinic acetylcholine receptor (M2R) [22]. Once autoantibodies have been generated, autoimmune-mediated neuroinflammatory responses would readily take place elsewhere. In fact, Beggs et al. recently demonstrated that the blood-brain barrier in the rat spinal cord is transiently compromised in response to peripheral nerve injury [6].

CRPS symptoms usually spread to other areas of the body in a contiguous fashion. However, a noncontiguous pattern also can occur [45]. A study of the spreading pattern of CRPS symptoms by van Rijn found that spontaneous spread generally follows a contralateral or ipsilateral pattern, whereas diagonal spread is rare and generally preceded by a new trauma [46].

\* Corresponding author. Address: Department of Hand Surgery, Graduate School of Nagoya University, 65 Tsurumai-cho, Showa-ku, Nagoya 466-8550, Japan. Tel.: +81 52 741 2111; fax: +81 52 744 2785.

E-mail address: [hideyuki@circus.ocn.ne.jp](mailto:hideyuki@circus.ocn.ne.jp) (H. Ota).

A recent review by Cooper referred to paths of spread for neuroinflammation in the CNS as neuroinflammatory tracks, stating that numerous studies have tried to elucidate the mechanisms of spread by looking at functional and pathological changes in the nervous system [14]. However, little research appears to have shed light on the detailed mechanisms of spread for musculoskeletal manifestations.

Another mysterious issue about CRPS is the interrelationship between immobilization and triggering of CRPS. Immobilization is a widely recognized factor predisposing to the development of CRPS, with nearly half of CRPS sufferers in one study having a history of medically imposed immobilization. Terkelsen demonstrated that just 4 weeks of cast immobilization can cause transient changes in skin temperature, mechanosensitivity, and thermosensitivity, as well as changes in capsaicin-induced neurogenic inflammation [41,42]. Pepper et al. meticulously observed patients who had undergone elective hand surgery followed by cast immobilization and demonstrated increased sensitivity to punctuate, pressure, and cold stimuli, as well as vascular and trophic changes in the operated hands of most patients [31]. In addition, they conducted skin biopsies in the affected areas and found increased expressions of interleukin (IL) 6, tumor necrosis factor (TNF)  $\alpha$ , and the mast cell marker tryptase [31]. However, whether immobilization is actually involved in triggering clinically significant CRPS and exaggeration of symptoms such as spread to contingent areas remains unclear. This study investigated these issues by looking at functional, biochemical, and histological alterations in the affected parts, including contiguous zones, using a rodent model.

## 2. Methods

### 2.1. Experimental animal model

Ninety-four male Wistar rats (Japan SLC, Hamamatsu, Japan) were used in this study, at 10 weeks old with a mean weight of 350 g. Rats were housed in groups of 3 in plastic cages. Animals were allowed to acclimatize to the laboratory environment for 7 days before study initiation, and acclimatization sessions for the behavioral experiment were carried out on these days. Rats were housed with a light-dark cycle (12 hours light/12 hours dark) and kept in a temperature-controlled room (23°C) with ad libitum access to food and water. This study was conducted with the approval of the local animal ethics committee in accordance with the Regulations for Animal Experiments at Nagoya University (permission no. 21357), the Animal Protection and Management Law of the Japanese Government (no. 105), and Ethical Issues of the International Association for the Study of Pain (IASP) [49]. Spinal nerve ligation (SNL) was used as the model of neuropathic pain [21]. In brief, animals were anesthetized with an intraperitoneal injection of sodium pentobarbital (50 mg/kg). The left L5 nerves were exposed by removing a small piece of the paravertebral muscle and part of the left spinous process of the L5 vertebra. The left L5 spinal nerves were then carefully isolated and tightly ligated with 4-0 nylon. The diaphyses of the left femur and tibia were exposed through individual longitudinal incisions, and a U-shaped hooked soft wire (diameter 0.9 mm) was inserted to internally fix the knee joint in maximum flexion (Fig. 1). The wound was closed with 4-0 nylon sutures. This study was conducted in a stepwise fashion. In the first step, 30 rats were used to demonstrate consecutive changes in the hind foot sensitivity up to 4 weeks after surgery. In the second stage, 54 rats (30 rats for gene and protein assays, 18 for histological assessments, and 6 to address the effect of anesthetics) were used to demonstrate the pathological mechanism of allodynia and knee contracture. Because all evaluations in this stage required killing animals, we conducted assessments only at 2 weeks after surgery to minimize the animal number at the ethics

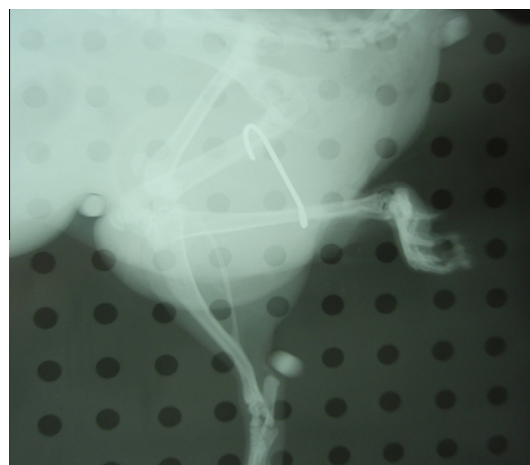


Fig. 1. Radiograph of the leg fixed with a U-shaped hooked wire, 0.9 mm in diameter.

committee's request. In the third stage, 10 rats were used to address the role of nerve growth factor (NGF).

### 2.2. Experimental groups

The normal group (NG) represents normal control subjects that did not receive any treatment. A sham operation group (ShG) was prepared by conducting exploration of the left L5 nerve root, femur, and tibia. The immobilization group (IG) was prepared by surgical exploration plus internal knee joint immobilization with a U-shaped hooked wire. The surgical neuropathy group (SG) was prepared by surgical exploration plus SNL. Finally, the surgical neuropathy + immobilization group (S+IG) was prepared by simultaneous SNL and knee joint immobilization.

### 2.3. Evaluation of mechanical allodynia

Comparisons were made between the 5 groups (6 rats each) for 4 weeks after surgery. Testing was performed only during the day portion of the circadian cycle (10:00 to 16:00). Rats were placed in a plastic cage with a mesh bottom. To assess allodynic responses to mechanical stimulus, calibrated Touch Test sensory monofilaments (Semmes-Weinstein von Frey Aesthesiometer; Muromachi Kikai, Tokyo, Japan) and the up-and-down method of testing were used [11]. Rats were tested and scored in sequential manner, starting with a 1.65 filament and increasing to a maximum of 6.65 (target force, 0.008 to 300 gf).

### 2.4. Evaluation of knee contracture

Comparisons were made between the 5 groups (6 rats each) at 2 weeks after surgery. The arthrometer used is shown in Fig. 2. The main components of the arthrometer are the peg board (a board perforated with regularly spaced holes into which pegs can be fitted), the fixation peg, the pulley, and the torque module. The rat is restrained to the arthrometer by the fixation peg. Torque levels for this arthrometer are determined through a preliminary experiment on a normal rat knee joint using 4 different weights (50 g, 100 g, 150 g, and 200 g). The test showed that more than 100 gf is needed to constantly obtain maximum passive knee extension on the arthrometer. As a result, 150 gf was applied in all experiments. To determine the tissue responsible for contracture, we conducted sequential measurements as follows. The rat was first anesthetized, and knee angle was measured under anesthesia (condition I). The rat was then killed with an overdose of anesthetic, and the leg was disarticulated at the hip joint, restrained on the arthrometer

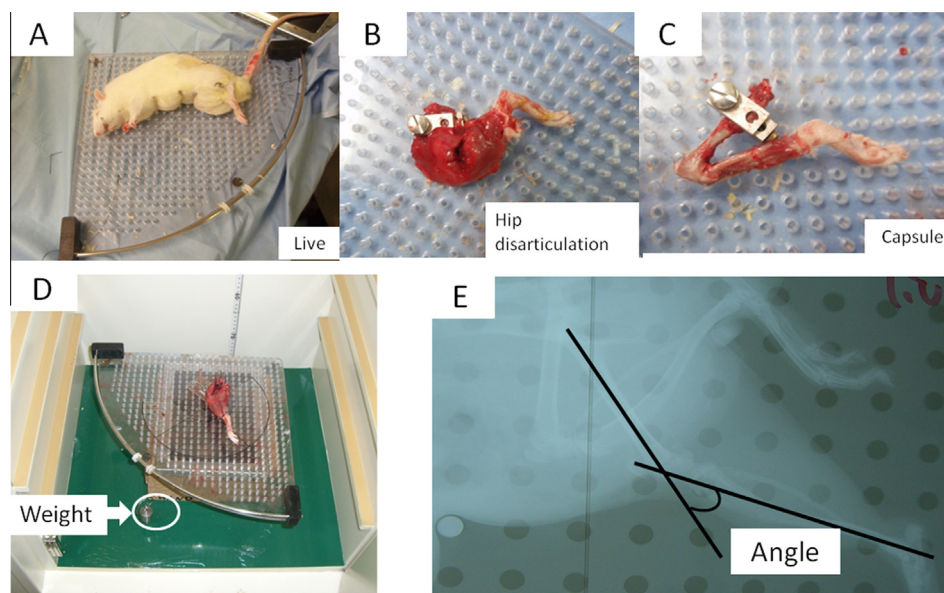


**Fig. 2.** Sequential measurement of maximum passive knee extension angle on the arthrometer. Condition I (A): the left leg was towed with a 150-g weight under general anesthesia so that the knee joint was maximally extended. Condition II (B, D): the left leg was harvested by hip disarticulation and the whole skin coverage was removed. The leg was fixed on the arthrometer, and passive knee joint angle measurement was conducted under 150-g weight traction. Condition III (C, D): all soft tissues except for ligaments and capsules were removed, and the leg was fixed and towed with a 150-g weight. Radiographs were taken on the arthrometer and digitized for accurate maximum passive knee extension angle measurement with ImageJ software.

in exactly the same way as in the first step, and measurement was again performed (condition II). Finally, all soft tissues except for ligaments and capsules of the knee joint were removed and measurement was repeated (condition III). We set up these 3 different conditions with the intention of examining the roles of pain-related spasticity (condition I), elements within the muscles (condition II), and the joint capsule and ligaments (condition III) on the development of contracture. Under each condition, we obtained radiographs of the whole leg for accurate measurement. The radiograph was digitized, and the angle of knee extension was measured using ImageJ software (National Institutes of Health, Bethesda, MD; ImageJ is in the public domain and can be downloaded from the ImageJ website: <http://rsb.info.nih.gov/ij/>). We conducted an additional experiment with 6 rats in each group to evaluate the contribution of supraspinal mechanisms to the development of contracture. In this experiment, measurement was carried out in exactly the same way, but rats were anesthetized with ketamine, an N-methyl-D-aspartate receptor antagonist that induces transient catalepsy by affecting dopaminergic systems, rather than with pentobarbital [15,19,48]. Rats were anesthetized with intraperitoneal injection of ketamine hydrochloride (75 mg/kg body weight) (Ketalar 10 mg/mL; Daiichi-Sankyo, Tokyo, Japan). After measurement in condition III, tissues were harvested for histological assessments and gene and protein expression analyses. Treatments for specimens of each assessment are described later.

### 2.5. Histochemistry

We assessed samples under light microscopy. Muscles were harvested in the mid-belly region and fixed in 4% phosphate-buffered paraformaldehyde at 4°C, dehydrated in a graded series of ethanol, infiltrated with xylene, and embedded in paraffin blocks. Five-micrometer-thick serial sections perpendicular to the direction of the muscle fiber were cut with a microtome and mounted on MAS-GP type A-coated glass slides (Matsunami Glass, Osaka, Japan). These sections were later dewaxed in xylene and rehydrated in descending grades of ethanol followed by a short 5-minute rinse under running water, then stained using hematoxylin and eosin and Masson modified trichrome stains to reveal the muscle architecture

and fibrosis components. To minimize bias during analyses, all observers were blinded to treatment group assignments. Mid-belly cross-sections were examined using a BX53F microscope (Olympus, Tokyo, Japan). Analysis was performed using a system comprising a video camera, automatic image analyzer, and ImageJ software. In each section, areas of connective tissue and muscle fiber were recorded by measuring optical density in a microscopic field at 200 $\times$  magnification. In calculating connective tissue area for each muscle, 5 fields were chosen from 1 section, 1 from the central area of the section and 4 from halfway between the center and periphery of the section. The amount of connective tissue in each section was expressed as a percentage of the total area of the field analyzed. The mean of the results from the 5 areas on each section was calculated, and this mean and the standard deviation were used as the fibrosis-area ratio (FAR). FAR can be confounded by physiological muscle atrophy after nerve injury, which would result in a relative increase in connective tissue element. To compensate for this drawback of FAR, we also conducted a qualitative assessment of muscle fibrosis with emphasis on differences in connective tissue distribution.

### 2.6. Immunohistochemistry

Immunohistochemical analysis was performed with transversely cut specimens of 5- $\mu$ m thickness to detect the expression pattern of NGF in muscles of both the area supplied by L5 and the surrounding areas. Tissue sections were cut using a tissue microtome and then mounted. After de-waxing and rehydration, slides were immersed in an antigen retrieval solution containing 10 mM sodium citrate hydrate for 30 minutes in a warm bath at a temperature of 97°C. Nonspecific staining of proteins was blocked overnight by nonspecific protein block (sc-548-p, 0.2 mg/mL; Santa Cruz Biotechnology, CA). Immunohistochemistry was performed using the standard method of diaminobenzidine (20 mg/mL) detection. All incubations were carried out at room temperature. The primary antibody was rabbit anti-NGF antibody (sc-548, 0.2 mg/mL; Santa Cruz Biotechnology) with phosphate-buffered saline at 1:100. Antibody was applied overnight after biotinylated multilink peroxidase agent with 0.3% H<sub>2</sub>O<sub>2</sub> for 30 minutes. The secondary antibody was goat anti-rabbit

immunoglobulin G (Histofine Simple Stain Rat MAX-PO(R); Nichirei Biosciences, Tokyo, Japan), with immersion in diaminobenzidine substrate for 10 minutes and washing in phosphate-buffered saline. Counterstaining was performed with Nuclear Fast Red (Kernechtrot) solution (Nuclear Fast Red; Sigma-Aldrich, St. Louis, MO) for 1 minute, washing in water, and dehydration by passing through graded ethanol and xylene solutions. Slides were coverslipped using NEO microscope cover glass (C024321; Matsunami Glass) mounted in a xylene-based medium (ENTELLAN neu; Merck, Darmstadt, Germany). In each batch of staining, we included both positive and negative controls to support the validity of the results.

### 2.7. Enzyme-linked immunosorbent assay (ELISA) for NGF, transforming growth factor (TGF)- $\beta$ 1, TNF- $\alpha$ , IL-1 $\beta$ , IL-6, calcitonin gene-related peptide (CGRP), and substance P (SP)

All ELISAs were conducted using frozen tissue samples. All samples were separated, aliquoted, diluted to the same protein concentration, and stored at  $-80^{\circ}\text{C}$  until further use. Concentrations of NGF, TNF- $\alpha$ , IL-1 $\beta$ , IL-6, CGRP, SP, and TGF- $\beta$ 1 in frozen tissues were measured using specific ELISA kits. The sensitivity of NGF (Abnova, Taipei, Taiwan) and TGF- $\beta$ 1 ELISA kits (Abnova) was  $<1$  pg/mL. TNF- $\alpha$ , IL-1 $\beta$ , IL-6, CGRP, and SP contents in samples were measured using ELISA kits for rat TNF- $\alpha$  (Ray Biotech, Norcross, GA), IL-1 $\beta$  (Abnova), IL-6 (Aviva Systems Biology, San Diego, CA), CGRP (Phoenix Europe GmbH, Karlsruhe, Germany), and SP (Phoenix Europe GmbH).

### 2.8. Anti-NGF antibody administration and quantitative gene expression assay with real-time polymerase chain reaction (PCR)

To clarify the role of NGF in producing musculoskeletal pain and its spontaneous spread into the contiguous area, we intraperitoneally administered neutralizing antibody against NGF (Sigma-Aldrich, St Louis, MO), at a dose of 1 mg/kg every 7 days after surgery. In this study, only the S + IG group was used. The level of mechanical allodynia in the plantar region was compared between rats receiving anti-NGF antibody ( $n = 5$ ) and those without ( $n = 5$ ) up to 14 days after surgery. At the end of the last assessment, animals were killed and the quadriceps femoris and hamstrings muscle were quickly harvested and immediately frozen in liquid nitrogen, then stored at  $-80^{\circ}\text{C}$  before the preparation of RNA. Total RNA was harvested, reverse transcribed, and assessed with real-time PCR to determine expression of NGF mRNA in the quadriceps femoris and hamstrings muscles. Real-time PCR was performed using the TaqMan Gene Expression Assay (Applied Biosystems, Foster City, CA) on an AB StepOne Real-Time PCR System (Applied Biosystems). For each gene, a set of primers and a probe were chosen from the Applied Biosystems list of TaqMan Gene Expression Assays. Expression of  $\beta$ -actin was used as an endogenous control for normalization, and nontransduced samples were used as calibrator controls. Data were then collected via the AB StepOne Real-Time PCR System and analyzed with the comparative CT method using SDS version 1.3.1 Relative Quantification software (Applied Biosystems, Foster City, CA). Effects of anti-NGF antibody on NGF production in each muscle also were assessed qualitatively by immunohistochemical staining with the method described previously.

### 2.9. Statistical analysis

Statistical analyses were performed using the Kruskal-Wallis test. All data are expressed as mean  $\pm$  SEM. Data were analyzed using SPSS version 20.0 (SPSS, Chicago, IL). Differences were considered significant for values of  $P < .05$ .

## 3. Results

### 3.1. Nerve injury induces allodynia that can be exaggerated by prolonged immobilization

The comparison between NG, ShG, and IG did not reveal any appreciable differences in threshold force value or patterns of change at any time point (Fig. 3). This indicates that neither surgical procedure nor 4-week immobilization induced mechanical hypersensitivity in the plantar region at an intensity high enough to be detected by the behavioral test used. On the other hand, addition of nerve injury constantly led to detectable mechanical allodynia in the plantar region. Threshold forces preoperatively and at 1, 2, and 4 weeks after surgery were  $42 \pm 16.8$  gf,  $97 \pm 6.1$  gf,  $75 \pm 3.0$  gf, and  $76 \pm 2.6$  gf in NG,  $44 \pm 5.7$  gf,  $8.7 \pm 3.3$  gf,  $18 \pm 5.1$  gf, and  $27 \pm 7.7$  gf in SG, and  $62 \pm 8.2$  gf,  $18 \pm 13.0$  gf,  $4.5 \pm 10.0$  gf, and  $7.7 \pm 16.2$  gf in S + IG, respectively. Rats in both SG and S + IG groups developed mechanical allodynia by 1 week after surgery that was maintained up to at least 4 weeks. An appreciable difference in the pattern of change was seen between these 2 groups (Fig. 3). In the former, mechanical allodynia peaked at 1 week and began to improve thereafter, whereas the latter showed little sign of improvement for the observed 4 weeks. Our results indicate that the combination of SNL and immobilization continues to lower and sustain the mechanical withdrawal thresholds a 2 and 4 weeks as compared with SNL alone, but this difference only reached the 0.06 level of significance with the cohorts of 6 rats in our study.

### 3.2. Prolonged immobilization induces muscle contracture that can be exaggerated by nerve injury

Radiological osteopenia was not observed at any time point in any group. The largest decrease in knee joint range of motion was observed after hip disarticulation in NG and ShG, suggesting that physiological tension of the bi-articular muscles provides the major restraint to knee motion. However, because there was no loss of range of motion between conditions II and III, uni-articular muscles contribute little to the restraint of knee motion. In addition, the lack of difference between NG/ShG and SG indicates that denervation does not stiffen muscle for the first 2 weeks. In contrast, a significant decrease was observed between

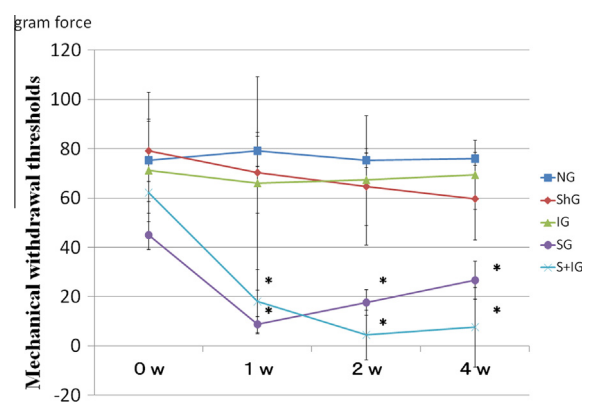


**Fig. 3.** Sequential changes of mechanical withdrawal thresholds measured by the von Frey hair test in each group. Blue line, normal group (NG); red line, sham operation group (ShG); green line, immobilization group (IG); purple line, surgical neuropathy group (SG); and aqua blue line, surgical neuropathy + immobilization group (S + IG). Data are presented as mean  $\pm$  SEM obtained from 6 rats. \* $P < .05$ . All asterisks show significant differences between each of the upper 3 groups and the lower group. The potential lower and sustained thresholds of S + IG when compared with SG alone tested at  $P = .06$  for the cohorts of 6 rats.

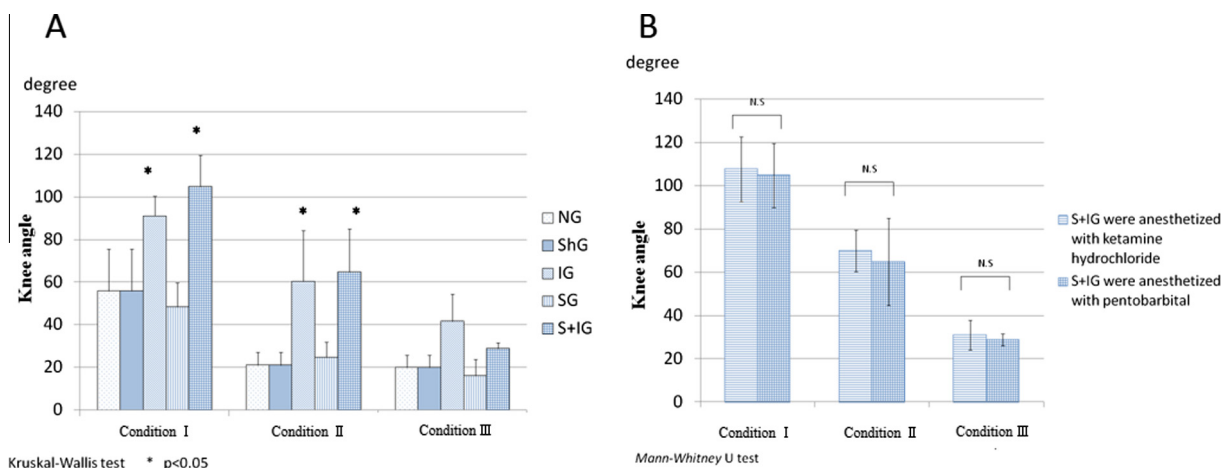


**Fig. 4.** (A) Passive extension angle of the knee in each condition. Empty bar, NG; solid bar, ShG; transverse parallel line pattern, IG; longitudinal parallel line pattern, SG; and cross-hatched line pattern, S + IG. Note that nerve injury alone does not cause any knee joint stiffness. In addition, an appreciable difference in the declining pattern seems evident between NG/ShG/SG and IG/S + IG. In the former, muscle fiber tension accounts for most of the knee joint stiffness, whereas the latter shows a sequentially declining pattern. \*Significant difference vs NG. (B) Comparison of passive extension angle of the knee between rats anesthetized with pentobarbital and those with ketamine under each condition. No significant differences were identified between the 2 groups under any of the conditions. NG, normal group; ShG, sham operation group; IG, immobilization group; SG, surgical neuropathy group; S + IG, surgical neuropathy + immobilization group.

conditions I and II/III in both IG and S + IG as compared with NG/ShG/SG (Fig. 4). This implies that development of severe neuropathic pain does not necessarily make bi-articular muscles stiff enough to restrict motion of the affected limb, and immobilization is necessary for the development of contracture.

The results of both behavioral testing and knee angle measurement have several important implications. First, sham operation has little effect on neuropathic pain or limb contracture. Second, allodynia and limb contracture are independent events in CRPS type II. Third, nerve injury and immobilization provide independent, additive contributions to both allodynia and limb

contracture. Taking these implications into consideration, the following assessments compared NG, SG, and S + IG, so as to clarify the roles of nerve injury and immobilization on the development and spread of CRPS symptoms and to elucidate the underlying mechanisms.

### 3.3. Muscle fiber degeneration and fibrosis is the cause of muscle contracture in CRPS

Histochemical assessment was performed with samples harvested 2 weeks after surgery. FAR was 3.7% ± 0.3% in NG, ShG,

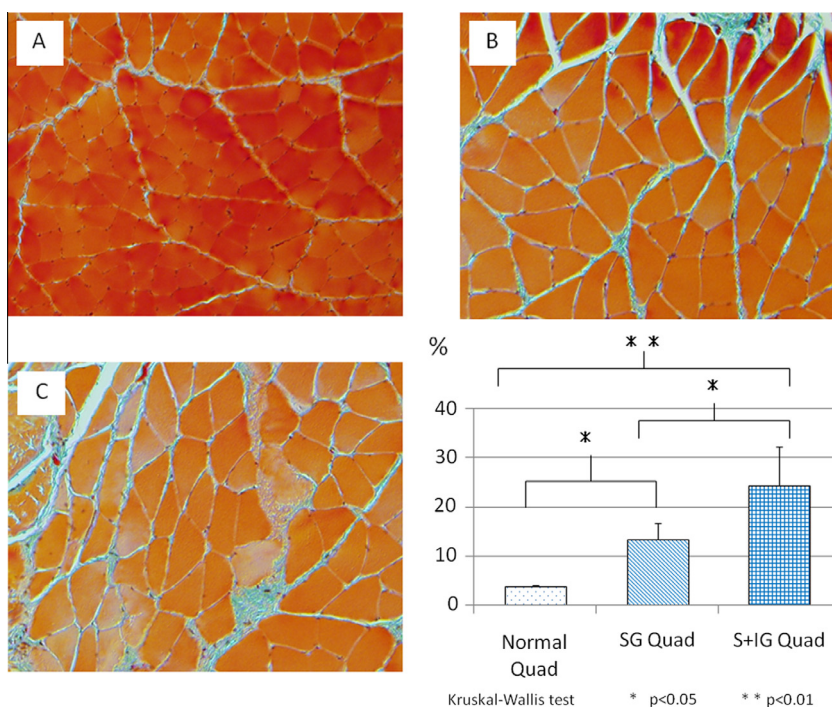


**Fig. 5.** Histochemical analysis of the left quadriceps femoris muscle with Masson modified trichrome stains at 2 weeks after surgery. (A–C) Representative specimens from NG (A), SG (B), and S + IG (C). Note the nonhomogeneous staining of muscle fibers in S + IG, which suggests muscle fiber degeneration and associated fibrosis. Bar graph shows FARs at 2 weeks after surgery. Values are expressed as mean ± SEM. \*\**P* < .01. \**P* < .05. Quad, quadriceps femoris muscle. NG, normal group; IG, immobilization group; SG, surgical neuropathy group; FAR, fibrosis area ratio; S + IG, surgical neuropathy + immobilization group.

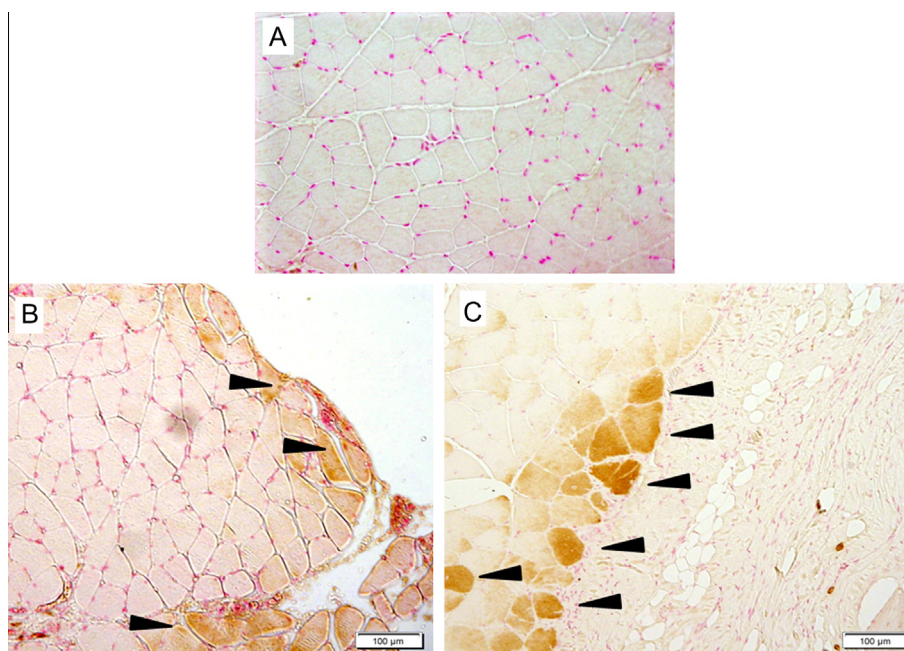


**Fig. 6.** Immunohistochemical staining for NGF in the left quadriceps femoris muscle harvested at 2 weeks. Black arrows indicate positively stained muscle fibers. (A–C) Representative specimens from NG (A), SG (B), and S + IG (C). Note that NGF is expressed mostly by muscle fibers located superficially. NG, normal group; IG, immobilization group; SG, surgical neuropathy group; NGF, nerve growth factor; S + IG, surgical neuropathy + immobilization group.

and IG;  $13.4\% \pm 3.3\%$  in SG; and  $24.4\% \pm 7.7\%$  in S + IG, respectively; all of these values differed significantly from each other (Fig. 5). Although both SG and S + IG showed significantly higher FAR compared with NG, a striking difference in the nature of fibrosis was seen between groups. In SG, the increase in FAR reflected hyperplasia of the epimysium, perimysium, and endomysium, whereas many muscle fibers had degenerated and been replaced by fibrous tissue in S + IG. Considering the fact that SG did not show any limb contracture under any of the 3 measurement conditions, muscle fiber degeneration seems to be prerequisite for the development of limb contracture.

#### 3.4. Immunohistochemistry

Immunohistochemical staining clearly shows that although muscle fibers in NG produce little NGF, some muscle fibers, particularly those located superficially, show high expression of NGF in CRPS models. NGF-producing muscle fibers were found not only in denervated muscles such as the tibialis anterior, but also in innervated muscles in the contiguous areas (Fig. 6). Considering that the quadriceps does not receive any axons from the L5 nerve root [39], this result suggests the spread of NGF production beyond the myotome of the injured nerve.

#### 3.5. NGF and other mediators of neurogenic inflammation are highly expressed, not only by denervated muscles, but also by innervated muscles in the contiguous area in CRPS

Quantitative assessment by ELISA showed that NGF levels increased in the order of S + IG, SG, and NG, with significant differences between each group for all assessed muscles (Fig. 7A). Considering the widespread expression of NGF in the CRPS type II model, we next studied expression of inflammatory mediators and neuropeptides that are known to corroborate with NGF in neurogenic inflammation in quadriceps femoris muscle on the denervated side. Both SP and CGRP are known to trigger neurogenic inflammation [34,35,47], increasing in the order of S + IG, SG, and NG with significant differences from each other (Figs. 7B, C).

Regarding proinflammatory cytokines, expressions of TNF- $\alpha$ , IL-1 $\beta$ , and IL-6 elevated again in the order of S + IG, SG, and NG with significant differences between each other (Figs. 7D, F). These results suggest that neuroinflammatory mechanisms are involved in the spontaneous spread of pain in CRPS, with both pain and inflammation worsening if the limb is immobilized.

#### 3.6. Neutralizing antibody alleviates allodynia in CRPS

As seen in Fig. 8A, mechanical allodynia was significantly alleviated by repeated administration of anti-NGF antibody in the quadriceps femoris of S + IG at all time points. In addition, quantitative analysis of NGF gene expression showed significant downregulation in using anti-NGF antibody groups (Figs. 8B, C), suggesting that treatments targeting NGF may not only suppress allodynia, but also inhibit the spread of symptoms.

#### 3.7. TGF- $\beta$ is involved in the development and spread of contracture in CRPS

To address the molecular mechanisms of the fibrosis observed in muscles, we quantified levels of TGF- $\beta$ , a multifunctional cytokine that plays central roles in wound healing [9] and tissue repair. Excessive expression of TGF- $\beta$  leads to a pathological excess of tissue fibrosis in the quadriceps femoris muscle in many diseases [8]. Again, we found significant increases in TGF- $\beta$  production in the order of S + IG, SG, and NG (Fig. 7G). This result is consistent with histochemical analyses, in that fibrosis takes place even in innervated muscles adjacent to the denervated area and the tissue response can be significantly enhanced by immobilization. These results indicate a central role of this cytokine in the development and spread of contracture in CRPS type II.

## 4. Discussion

CRPS is a chronic neuropathic pain disorder distinguished by significant autonomic features [10]. Although CRPS is currently subdivided into 2 categories by the IASP depending on the absence

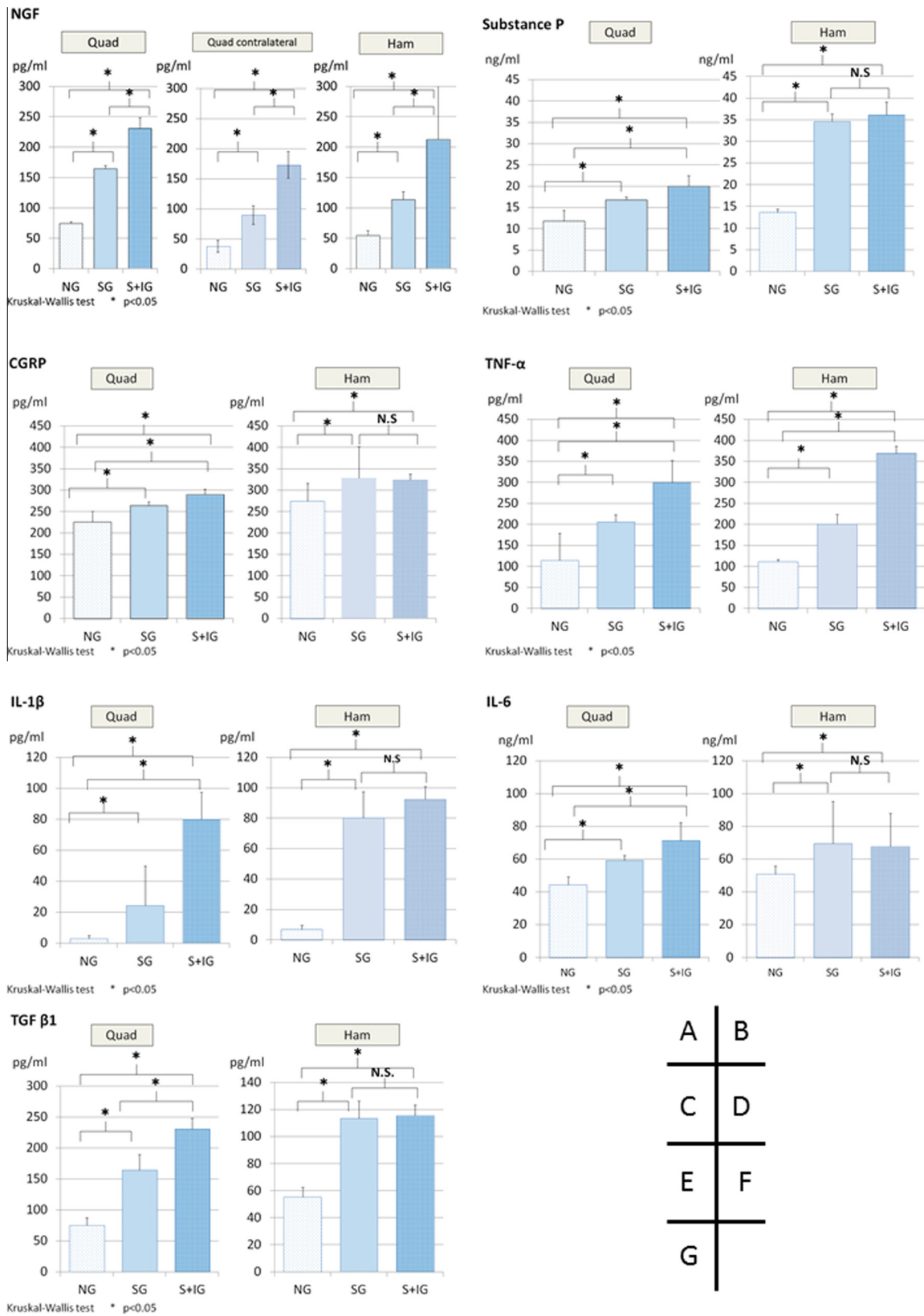


**Fig. 7.** Each panel shows the results of immunoassay for NGF (A), substance P (B), CGRP (C), TNF-α (D), IL-1β (E), IL-6 (F), and TGF-β1 (G) in the left quadriceps (Quad), right quadriceps femoris muscle (Quad contralateral), and hamstrings, all harvested at 2 weeks. Data are expressed as mean ± SEM (n = 6). \*P < .05. NS, no statistical significance. NGF, nerve growth factor; CGRP, calcitonin gene-related peptide; TNF, tumor necrosis factor; IL, interleukin; TGF, transforming growth factor.

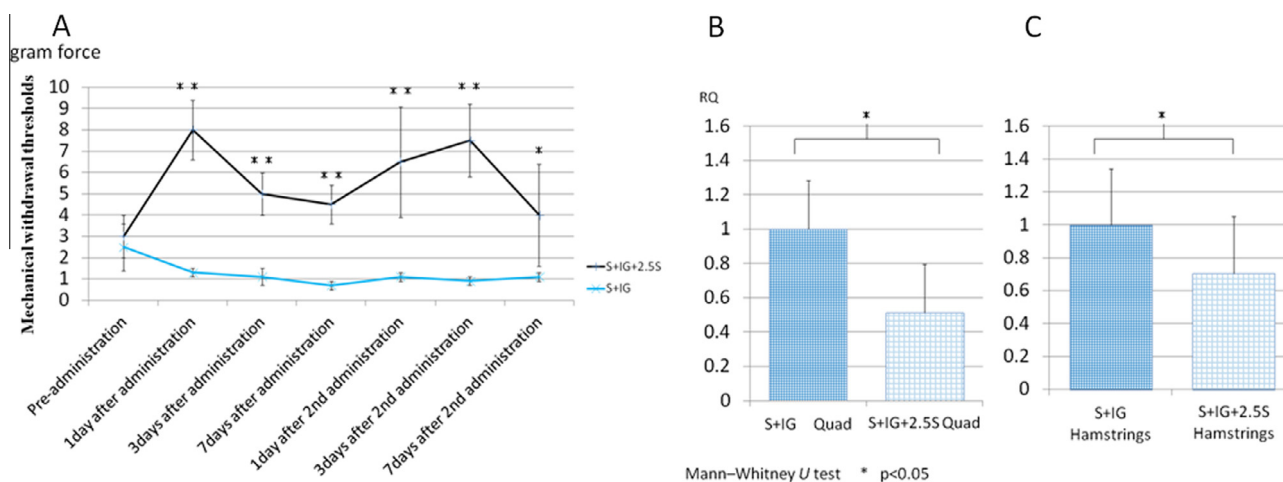


**Fig. 8.** The line graph (A) shows serial changes in mechanical withdrawal thresholds in group S + IG after surgery. Black line, results of rats with NGF-neutralizing antibody treatment (S + IG + 2.5 S); blue line, results of rats without (S + IG). Bar graphs show NGF mRNA expression levels as measured by real-time PCR. Aqua blue bar, S + IG + 2.5 S; blue bar, S + IG. (B) Expression level of NGF mRNA in the quadriceps femoris muscle. (C) Those in the hamstrings. \*\* $P < .01$ . \* $P < .05$ . NGF, nerve growth factor; S + IG, surgical neuropathy + immobilization group; PCR, polymerase chain reaction.

or presence of nerve injury, little evidence exists to support such subclassification [3,10]. In fact, the notion that nerve damage is involved even in CRPS type I is gaining credence [1,7,28].

The present experimental study attempted to demonstrate the pathological mechanisms underlying the motor disorders and musculoskeletal manifestations seen in CRPS. We also examined the effects of immobilization on CRPS. We used a modified Chung model in which the L5 root was completely ligated [24,33]. The rationale behind using this model was that, although this is a general neuropathic pain model, it is widely accepted as a CRPS model that can produce allodynia, hyperalgesia, edema, temperature changes, and trophic changes similar to CRPS [10]. In contrast to the original model [21] in which the nerve root received incomplete or ambiguously defined injury, this modified model offers consistent nerve injury. We thought this would be advantageous to study the spontaneous spread of symptoms that is often discussed without clear definition, resulting in significant confusion and misunderstanding. Using this model with consistent initial symptoms strictly confined to the area supplied by the L5 root, any symptoms appearing beyond the L5 territory can be regarded as the spreading phenomenon. On the other hand, several limitations to this animal experiment need to be acknowledged. First, CRPS in clinical practice is usually triggered not by an internally applied fixation device, but by an externally applied cast that causes skin irritation and thermal changes in addition to preventing movement of involved joints [41,42]. We therefore could not address the roles that these inputs may also play in pain exacerbation. Second, we used male rats in this experiment according to the original description by Kim and Chung. However, accumulating evidence has clearly shown a strong female predominance for CRPS. Therefore, we will continue our investigation using female rats in future studies. Third, evaluation was performed up to 4 weeks in this experiment, which is not strictly comparable with the usual clinical situation in which patients are generally seen after more than 3 months. In fact, although we focused on musculoskeletal changes in CRPS and the underlying pathological mechanisms in this study, marked differences existed in the pathology observed both by us and by previous clinical studies. Hulsman analyzed muscles from the amputated extremities of CRPS type I patients and reported extensive and varied changes attributable both to disuse and neurogenic mechanisms [5,20]. Interestingly, our results indicated that combining SNL with immobilization may continue to lower and sustain the mechanical withdrawal thresholds at 2 and 4 weeks compared with SG alone.

When assessing the spontaneous spread of pain, researchers need to be very careful about definitions. According to Takahashi et al., who meticulously mapped rat sclerotomes using a retrograde neurotracer [39], pain reported by patients with radiculopathy does not follow dermatomes, but instead follows myotomes [38]. In fact, patients with lumbar radiculopathy usually report pain in the buttock, thigh, or leg, and less often in the foot and toes in common lumbar radiculopathy, and the painful area is usually accompanied by muscle tenderness.

Our experiment did not evaluate the spread of hyperalgesia directly, but instead studied the expression of NGF. NGF has recently been attracting much attention as a key substance involved in muscle hyperalgesia [4,23,32]. In the present study, the finding that NGF antibody temporarily ameliorated mechanical hyperalgesia in the sole confirmed the role of NGF in sensitization. Similar results have been reported by others using a CRPS type I model [17,35]. Hayashi et al. recently conducted repeated intramuscular injections of NGF to 12 healthy human subjects and showed that daily injection induced progressive muscle hyperalgesia, facilitated temporal summation, and expanded pain areas [18]. Our present study assessed NGF production in muscles by measuring protein expression with immunohistochemistry and ELISA, both of which confirmed significantly higher expression in the CRPS model as compared with a sham control. As shown earlier, NGF levels seemed related to the severity of both hyperalgesia and joint contracture. Given that a report by the IASP found that motor/trophic symptoms form a factor clearly distinct from the pain/sensation factor by principal component factor analysis [16], these 2 factors are highly unlikely to share pathological mechanisms. From a myotome perspective, enhanced NGF expression in the quadriceps muscles should be noted. According to Takahashi, the quadriceps muscles are included within the L3 and L4 myotome [37,40]. High expression of NGF in quadriceps muscles thus indicates a spontaneous spread of pain/sensory symptoms beyond the injured nerve territory. Furthermore, enhanced NGF expression was observed in CRPS models not only on the ipsilateral side, but also on the contralateral side, although a significant difference in expression level exists between the 2 sides.

Some recent studies have suggested the possibility that inflammatory mechanisms might contribute, at least in the acute phase of CRPS [2,12]. In fact, some clinical research has shown significant increases in proinflammatory cytokines such as TNF- $\alpha$ , IL-1 $\beta$ , and IL-6 in local blister fluid, circulating plasma, and cerebrospinal fluid [13,25,44]. Wei et al. studied the interrelationship between

these proinflammatory cytokines and NGF and the roles of these molecules in the generation of CRPS symptoms using a rat CRPS type I model involving tibial fracture and immobilization [34,35,47]. Expressions of these molecules on the affected skin were all found to be upregulated by SP through its receptor, NK1. According to Wei et al. neuropeptides including SP and CGRP are involved in nociceptive sensitization, vascular components, and edema formation, but not in bone-related changes [47]. They also found the following. First, NGF antibody could alleviate nociceptive changes, but could not affect vascular components. Second, blockade of NGF activity inhibited nociceptive sensitization, but not the production of other inflammatory mediators in the fracture model [35]. These data support their premise that SP and CGRP act as intermediate mediators in the development of inflammatory pain via other downstream substances such as cytokines, and NGF seemed to be the most plausible candidate responsible for nociceptive sensitization. The present study quantitatively assessed expression of these molecules in muscles and confirmed enhanced expression in a CRPS type II model. Addition of immobilization to CRPS was found to significantly increase expression of these substances even in the quadriceps muscles, and significantly aggravated both mechanical and thermal hyperalgesia. Overall, NGF seems highly likely to be responsible for hyperalgesia in both skin and deep tissues, including muscles, and is directly involved in spontaneous spread beyond the myotome via NGF, and immobilization aggravates pain/sensory factor of CRPS by upregulating NGF production.

Regarding motor/trophic symptoms, what we assessed in this experiment was the severity of joint contracture, and we did not conduct any quantitative assessments of musculoskeletal manifestations. The reasons for this are twofold. First, quantitative assessment of musculoskeletal manifestations in rats is extremely difficult. Second, although dystonia is the most common type of musculoskeletal manifestation associated with CRPS, it is clearly different from primary dystonia [26,27]. Primary dystonia is typically characterized by prolonged twisting and repetitive movements [43]. In contrast, the dystonia seen in CRPS features abnormal postures, known as fixed dystonia [26]. Therefore, on assessment, researchers need to carefully discriminate between fixed dystonia in which joint motion is restricted due to sustained contraction of surrounding muscles and joint contracture representing loss of joint motion due to tightness of capsule. For this purpose, we measured passive range of motion under 3 different conditions: under anesthesia, after hip disarticulation, and after removal of all muscles around the knee joint. One weakness of this study was that we could not evaluate knee joint motion in conscious rats. This means that we could not detect any changes in muscle tone unless indissoluble structural changes occur. The CRPS without immobilization group would thus have shown joint contracture if we had performed assessments with the rats awake. Still, very interesting findings were obtained in this experiment. Loss of joint motion in the CRPS model at 2 weeks was not due to tightness of joint capsule, but rather to the tightness of muscles around the knee. Histochemical analysis clearly showed that immobilization alone did induce interstitial fibrosis as early as 2 weeks, as reported by others [13]. More importantly, the presence of CRPS significantly enhances interstitial fibrosis in muscles. Considering these findings, fixed dystonia may not be an appropriate term for the abnormal postures in CRPS. This view is supported by a recent neurophysiological study that demonstrated clearly that chronic CRPS patients with abnormal postures do not show electrophysiological characteristics of dystonia [5]. To reveal the underlying pathological mechanisms, we quantitatively measured activity of TGF- $\beta$ , a multifunctional cytokine that plays a central role in wound healing and is involved in tissue fibrosis [9]. This

result was consistent with histochemical assessments, in that TGF- $\beta$  expression was highest in S + IG, followed by SG. The implication of these results is that immobilization not only accelerates hyperalgesia and spread of pain, but also induces muscle fibrosis.

### Conflict of interest statement

The authors declare that they have no conflict of interest.

### Acknowledgments

This study was supported by Japan Society for the Promotion of Science (JSPS), Grants-in-Aid for Scientific Research (KAKENHI) grant number 24791537. The authors did not and will not receive any benefits from any commercial party related directly or indirectly to the subject of this article.

### References

- [1] Albrecht PJ, Hines S, Eisenberg E, Pud D, Finlay DR, Connolly MK, Paré M, Davar G, Rice FL. Pathologic alterations of cutaneous innervation and vasculature in affected limbs from patients with complex regional pain syndrome. *PAIN*® 2006;120:244–66.
- [2] Alexander GM, van Rijn MA, van Hilten JJ, Perreault MJ, Schwartzman RJ. Changes in cerebrospinal fluid levels of pro-inflammatory cytokines in CRPS. *PAIN*® 2005;116:213–9.
- [3] Allen G, Galer BS, Schwartz L. Epidemiology of complex regional pain syndrome: a retrospective chart review of 134 patients. *PAIN*® 1999;80:539–44.
- [4] Amano T, Yamakuni T, Okabe N, Sakimura K, Takahashi Y. Production of nerve growth factor in rat skeletal muscle. *Neurosci Lett* 1991;132:5–7.
- [5] Bank PJM, Peper C, Lieke E, Marinus J, Beek PJ, van Hilten JJ. Deficient muscle activation in patients with Complex Regional Pain Syndrome and abnormal hand postures: an electromyographic evaluation. *Clin Neurophysiol* 2013;124:2025–35.
- [6] Beggs S, Liu XJ, Kwan C, Salter MW. Peripheral nerve injury and TRPV1-expressing primary afferent C-fibers cause opening of the blood-brain barrier. *Mol Pain* 2010;6:74.
- [7] Birklein F, Schmelz M. Neuropeptides, neurogenic inflammation and complex regional pain syndrome (CRPS). *Neurosci Lett* 2008;437:199–202.
- [8] Branton MH, Kopp JB. TGF-beta and fibrosis. *Microbes Infect* 1999;1:1349–65.
- [9] Braus DF, Krauss JK, Strobel J. The shoulder-hand syndrome after stroke: a prospective clinical trial. *Ann Neurol* 1994;36:728–33.
- [10] Bruehl S. An update on the pathophysiology of complex regional pain syndrome. *Anesthesiology* 2010;113:713–25.
- [11] Chaplan SR, Bach FW, Pogrel JW, Chung JM, Yaksh TL. Quantitative assessment of tactile allodynia in the rat paw. *J Neurosci Methods* 1994;53:55–63.
- [12] Christensen K, Jensen EM, Noer I. The reflex dystrophy syndrome response to treatment with systemic corticosteroids. *Acta Chir Scand* 1982;148:653–5.
- [13] Chung MS, Baek GH, Oh JH, Lee YH, Bin SW, Gong HS. The effect of muscle length and excursion on muscle contracture after tendon injury: a study in rabbit soleus muscles. *Injury* 2007;38:1139–45.
- [14] Cooper MS, Clark VP. Neuroinflammation, neuroautoimmunity, and the comorbidities of complex regional pain syndrome. *J Neuroimmune Pharmacol* 2013;8:452–69.
- [15] Hance AJ, Winters WD, Quam DD, Benthuyens JL, Cadd GG. Catalepsy induced by combinations of ketamine and morphine: potentiation, antagonism, tolerance and cross-tolerance in the rat. *Neuropharmacology* 1989;28:109–16.
- [16] Harden RN, Bruehl S, Galer BS, Saltz S, Bertram M, Backonja M, Gayles R, Rudin N, Bhugra MK, Stanton-Hicks M. Complex regional pain syndrome: are the IASP diagnostic criteria valid and sufficiently comprehensive? *PAIN*® 1999;83:211–9.
- [17] Hayashi K, Ozaki N, Kawakita K, Itoh K, Mizumura K, Furukawa K, Yasui M, Hori K, Yi SQ, Yamaguchi T, Sugiura Y. Involvement of NGF in the rat model of persistent muscle pain associated with taut band. *J Pain* 2011;12:1059–68.
- [18] Hayashi K, Shiozawa S, Ozaki N, Mizumura K, Graven-Nielsen T. Repeated intramuscular injections of nerve growth factor induced progressive muscle hyperalgesia, facilitated temporal summation, and expanded pain areas. *PAIN*® 2013;154:2344–52.
- [19] Heitz CR, Bence JR. Ketamine-induced catalepsy during adult sedation in the emergency department. *J Emerg Med* 2013;44:e243–5.
- [20] Hulsman NM, Geertzen JH, Dijkstra PU, van den Dungen JJ, den Dunnen WF. Myopathy in CRPS-I: disuse or neurogenic? *Eur J Pain* 2009;13:731–6.
- [21] Kim SH, Chung JM. An experimental model for peripheral neuropathy produced by segmental spinal nerve ligation in the rat. *PAIN*® 1992;50:355–63.
- [22] Kohr D, Singh P, Tschernatsch M, Kaps M, Pouokam E, Diener M, Kummer W, Birklein F, Vincent A, Goebel A, Wallukat G, Bles F. Autoimmunity against the  $\beta 2$  adrenergic receptor and muscarinic-2 receptor in complex regional pain syndrome. *PAIN*® 2011;152:2690–700.

- [23] Lewin GR, Mendell LM. Nerve growth factor and nociception. *Trends Neurosci* 1993;16:353–9.
- [24] Li Y, Dorsi MJ, Meyer RA, Belzberg AJ. Mechanical hyperalgesia after an L5 spinal nerve lesion in the rat is not dependent on input from injured nerve fibers. *PAIN®* 2000;85:493–502.
- [25] Maihöfner C, Handwerker HO, Neundörfer B, Birklein F. Mechanical hyperalgesia in complex regional pain syndrome: a role for TNF-alpha? *Neurology* 2005;65:311–3.
- [26] Munts AG, Mugge W, Meurs TS, Schouten AC, Marinus J, Moseley GL, van der Helm FC, van Hilten JJ. Fixed dystonia in complex regional pain syndrome: a descriptive and computational modeling approach. *BMC Neurol* 2011;11:53.
- [27] Neychev VK, Gross RE, Lehericy S, Hess EJ, Jinnah HA. The functional neuroanatomy of dystonia. *Neurobiol Dis* 2011;42:185–201.
- [28] Oaklander AL, Rissmiller JG, Gelman LB, Zheng L, Chang Y, Gott R. Evidence of focal small-fiber axonal degeneration in complex regional pain syndrome-I (reflex sympathetic dystrophy). *PAIN®* 2006;120:235–43.
- [29] Ochoa JL, Verdugo RJ. Reflex sympathetic dystrophy. A common clinical avenue for somatoform expression. *Neurol Clin* 1995;13:351–63.
- [30] Parkitny L, McAuley JH, Di Pietro F, Stanton TR, O'Connell NE, Marinus J, van Hilten JJ, Moseley GL. Inflammation in complex regional pain syndrome: a systematic review and meta-analysis. *Neurology* 2013;80:106–17.
- [31] Pepper A, Li W, Kingery WS, Angst MS, Curtin CM, Clark JD. Changes resembling complex regional pain syndrome following surgery and immobilization. *J Pain* 2013;14:516–24.
- [32] Pezet S, McMahon SB. Neurotrophins: mediators and modulators of pain. *Annu Rev Neurosci* 2006;29:507–38.
- [33] Ringkamp M, Eschenfelder S, Grethel EJ, Häbler HJ, Meyer RA, Jänig W, Raja SN. Lumbar sympathectomy failed to reverse mechanical allodynia- and hyperalgesia-like behavior in rats with L5 spinal nerve injury. *PAIN®* 1999;79:143–53.
- [34] Sabsovich I, Guo TZ, Wei T, Zhao R, Li X, Clark DJ, Geis C, Sommer C, Kingery WS. TNF signaling contributes to the development of nociceptive sensitization in a tibia fracture model of complex regional pain syndrome type I. *PAIN®* 2008;137:507–19.
- [35] Sabsovich I, Wei T, Guo TZ, Zhao R, Shi X, Li X, Yeomans DC, Klyukin M, Kingery WS, Clark JD. Effect of anti-NGF antibodies in a rat tibia fracture model of complex regional pain syndrome type I. *PAIN®* 2008;138:47–60.
- [36] Stone J, Edwards MJ. How “psychogenic” are psychogenic movement disorders? *Mov Disord* 2011;26:1787–8.
- [37] Takahashi Y. Three dimensional structure of spinal nerves in the thoracolumbar body trunk. *Jpn J Rehabil Med* 2008;45:296–300 [in Japanese].
- [38] Takahashi Y. Visible low back pain: a hypothetic somatosensory structure map for the diagnosis of musculoskeletal pain. Tokyo: Nankodo; 2012 [in Japanese].
- [39] Takahashi Y, Ohtori S, Takahashi K. Human map of the segmental sensory structure (“sensoritomes”) in the body trunk and lower extremity. *Pain Res* 2008;23:133–41 [in Japanese].
- [40] Takahashi Y, Ohtori S, Takahashi K. Sclerotomes in the thoracic and lumbar spine, pelvis, and hindlimb bones of rats. *J Pain* 2010;11:652–62.
- [41] Terkelsen AJ, Bach FW, Jensen TS. Experimental forearm immobilization in humans induces cold and mechanical hyperalgesia. *Anesthesiology* 2008;109:297–307.
- [42] Terkelsen AJ, Bach FW, Jensen TS. Experimental forearm immobilization in humans reduces capsaicin-induced pain and flare. *Brain Res* 2009;1263:43–9.
- [43] Tinazzi M, Fiorio M, Fiaschi A, Rothwell JC, Bhatia KP. Sensory functions in dystonia: insights from behavioral studies. *Mov Disord* 2009;24:1427–36.
- [44] Uçeyler N, Eberle T, Rolke R, Birklein F, Sommer C. Differential expression patterns of cytokines in complex regional pain syndrome. *PAIN®* 2007;132:195–205.
- [45] van Hilten JJ, van de Beek WJ, Vein AA, van Dijk JG, Middelkoop HA. Clinical aspects of multifocal or generalized tonic dystonia in reflex sympathetic dystrophy. *Neurology* 2001;56:1762–5.
- [46] van Rijn MA, Marinus J, Putter H, Bosselaar SR, Moseley GL, van Hilten JJ. Spreading of complex regional pain syndrome: not a random process. *J Neural Transm* 2011;118:1301–9.
- [47] Wei T, Sabsovich I, Guo TZ, Shi X, Zhao R, Li W, Geis C, Sommer C, Kingery WS, Clark DJ. Pentoxifylline attenuates nociceptive sensitization and cytokine expression in a tibia fracture rat model of complex regional pain syndrome. *Eur J Pain* 2009;13:253–62.
- [48] Winters WD, Ferrar-Allado T, Guzman-Flores C, Alcaraz M. The cataleptic state induced by ketamine: a review of the neuropharmacology of anesthesia. *Neuropharmacology* 1972;11:303–15.
- [49] Zimmermann M. Ethical guidelines for investigations of experimental pain in conscious animals. *PAIN®* 1983;16:109–10.